Aerothermodynamic Parameter Estimation from Shuttle Thermocouple Data During Transient Flight Test Maneuvers

James K. Hodge* and David R. Audley†
Air Force Institute of Technology, Wright-Patterson Air Force Base, Ohio

Aerothermodynamic parameters are estimated from data of thermocouples imbedded in the Space Shuttle Orbiter Thermal Protection System (TPS). The new technique of analyzing transient flight test maneuvers is based on systems identification theory and has been applied to thermocouple data from the first four Shuttle re-entries. The primary purpose is to accomplish a rapid and safe envelope expansion for aerothermodynamic performance. The data reduction program correlates heating with variables such as angle of attack, sideslip, control surface deflection, and Reynolds number.

Nomenclature

A,B,C,D = coefficient matrices ($L \times L$)
c = specific heat
E = residual error (vector of length M)
F = likelihood function
G = Kalman gain (vector of length L)
H = matrix to define thermocouple location ($M \times L$)
h = enthalpy
I = identity matrix
J = conditional information matrix ($K \times K$)
K = total number of model parameters
k = thermal conductivity
L = total number of spatial node points
M = total number of thermocouples through the TPS
N = total number of thermocouple time samples
P = covariance matrix ($L \times L$)
Q = model error covariance matrix ($L \times L$)
$\bar{q}$ = heating rate ratio
q_0 = heating rate ratio intercept
$q_{(\cdot)}$ = heating ratio with respect to $(\cdot)$ derivative
$\dot{q}_r$ = reference heating rate
R = measurement error covariance
Re = freestream Reynolds number
R_c = time constant
S = score (vector of length K)
T_∞ = freestream temperature
t = time
U = temperature field (vector of length L)
$U_{\theta k}$ = sensitivity of U to kth parameter (vector of length L)
U_∞ = free-space temperature of radiation sink temperature
V_∞ = freestream relative velocity
W = error model for heat flux (vector of length L)
x = spatial depth
Y = thermocouple measurements (vector of length M)
α = angle of attack
β = angle of sideslip
Δ = forward difference operator
∇ = backward difference operator
δ = deflection angle
ϵ = emissivity
θ = model parameters (vector of length K)
λ = dummy variable
μ = measurement error (vector of length L)
ρ = density
Σ = summation or ensemble average
σ = Stefan-Boltzmann constant
τ = spatial error model (vector of length L)
Φ = transition matrix ($L \times L$)
ϕ = constant
Φ_B = thermal-conductivity factor
Δx_A = effective coating thickness

Superscripts

$(+)$ = a-posteriori update
$\hat{(\ )}$ = expected value
$(\bar{\ })$ = a-priori propagation
$(*)$ = best estimate
-1 = inverse

Subscripts

i,j = index of spatial node point
k = index of model parameter
m = index of thermocouple
n = index of time step
0 = initial condition
∞ = freestream condition

Introduction

AEROTHERMODYNAMIC parameters are estimated from flight test data of thermocouples imbedded in the Space Shuttle Orbiter Thermal Protection System (TPS). These parameters (primarily convective heating rate) are especially useful in expanding the envelope of the Orbiter to allow more severe re-entries during future operational missions. Angle of attack and axial center of gravity envelope expansion are primarily of interest. Higher cross range results from decreasing the current 40-deg angle of attack profile to a lower angle of attack. However, heating increases at some locations due to the lower angle of attack and also due to increased Reynolds number. Shifting the axial center of gravity aft also causes increased heating on the body flap and elevon control surfaces due to increased deflection angles. Due to plans for a limited number of fully instrumented test flights, it is desirable to expand the envelope and rapidly, but yet safely, before committing to lower angle of attack and to an aft center of gravity. A systematic technique to accomplish envelope expansion has been developed for aerothermodynamics, and applied to the Space Shuttle Orbiter TPS.

Requirements for the technique include an analytical model for the simulation of the heat transfer to a point on the TPS,

Received June 1, 1984; revision received Nov. 4, 1985.

*Major, USAF; Associate Professor of Aeronautics and Astronautics. Member AIAA.
†Major, USAF; Associate Professor of Mathematics.

flight test maneuvers which cause thermocouples imbedded near the surface of the TPS to respond sufficiently above noise levels, and a parameter-estimation program to reduce flight thermocouple data. The analytical model is divided into two parts, a heating model and a thermal model.

Simplified equations for convective heat rate, which will be referred to as heating models, were in use in off-line simulations for mission planning and sizing of the TPS.[1,2] The ratio of convective heat rate to a reference heat rate for several control points on the TPS was tabulated as a function of angle of attack. Surface temperature was approximated by assuming that the surface of the tile would reach equilibrium instantaneously with the convective heat rate, and radiate all the heat into space. Since the TPS at most locations has a very low conductivity, these assumptions provided a good approximation, as long as thermal transients could be neglected.

Another numerical method, referred to as a thermal model, was used in simulations to account for conduction and for calculation of bondline temperatures.[3] Effective TPS and structural thicknesses were used in the one-dimensional thermal model.[4] The thermal model required pressure and heat-rate time history inputs. Time histories for the temperatures at discrete node points in-depth through the TPS were thus simulated.

Heating models and thermal models for control points on the TPS were combined into one simulation, which was used for both off-line and for a real-time man in the loop-engineering simulator.[5] Heating rates were calculated by the convective heating model. Pressure, which was used only for thermal property determination, was calculated by various approximate theories such as Newtonian and tangent wedge, or by wind-tunnel-derived pressure coefficients. Parametric studies could then be conducted, especially for the transient response of surface thermocouples imbedded under a thin surface coating.

Thermocouple responses to some maneuvers which are used for aerodynamic performance[6,7] were then simulated. By suggesting a five-second duration hold at maximum and minimum angles of attack during a Push-Over-Pull-Up (POPU) maneuver, response of the lower-surface thermocouples was assured and a better response was obtained on some upper-surface thermocouples. Envelope expansion to lower and higher angle of attack could be accomplished. A similar flap maneuver for center of gravity envelope expansion was also suggested.

Parametric studies were conducted with the simulator to identify thermal parameters which would have a major influence on the heating rate at the surface of the Shuttle TPS. Thermal parameters which were identified included the surface emissivity and the effective coating depth of surface thermocouples. Parameters for the heating model were chosen to be the magnitude (or intercept) at a given reference condition such as zero angle of attack, and derivative (or slope) with respect to each variable such as angle of attack. Thermocouple samples were simulated during POPU maneuvers using manual piloting techniques. The simulated thermocouple samples were distorted with noise and with errors in the parameters.

A data-reduction program for the thermocouple data and transient maneuvers was developed and referred to as heating estimation. The heating and thermal models were used to predict the expected thermocouple responses with initial guesses for parameters. A maximum-likelihood criterion with a Newton-Raphson iteration was then used to obtain a best estimate for the parameters. However, since thermocouple measurements are not available for all state variables or nodes, a Kalman estimator was also required for updating the temperature at nodes where measurements are not available. This heating-estimation technique was proven[5] by using simulated surface thermocouple data. The program was also applied to thermocouple data for a High-Temperature-Reusable-Surface-Insulation article (HRSI) in a wind tunnel test,[8] and also to telemetered thermocouple data from the first Space Transportation System (STS-1) re-entry of the Orbiter.[5] No flight test maneuvers were performed on the first flight, however.

The first flight test maneuvers were performed on the second Shuttle re-entry (STS-2). A POPU maneuver was performed at approximately Mach 20. Three flap maneuvers were performed at aproximately Mach 21, 16, and 12. Analysis of lower surface HRSI thermocuple data from an on-board recorder was successful at numerous locations.[9,10] Results were also obtained at a point on the outboard elevon surface (HRSI) and on the Orbital-Maneuvering System (OMS) pod on the upper surface, where nomex felt Flexible RSI or FRSI is located. These points were important for envelope expansion, and their results from the heating estimation will be presented.

No flight test maneuvers of interest were performed on the third flight (STS-3), and two pull-up-push-over (POPU) maneuvers were performed on the fourth flight (STS-4) at approximately Mach 12 and 8. Unfortunately, only telemetered thermocouple data which began during the Mach 12 maneuver were obtained. Data from a plug of five in-depth thermocouples in the TPS at one point on the lower surface have been analyzed by the heating estimation program for the first time for these maneuvers. Angle-of-attack derivatives for both laminar and turbulent flow are estimated. Thus, Reynolds number trends and derivatives can be estimated.

The aerothermal parameters and the mathematical equations for the heating and thermal models will be summarized first in the next section. These parameters and equations are used in the simulator and in the heating estimation program. The systems identification theory used in the heating estimation technique is verified using simulated thermocouple data with known parameters. Then, results from flight test maneuvers from the second and fourth Space Shuttle flights are presented for three locations.

Heating and Thermal Models

Both the flight simulator and heating-estimation program require suitable simulation parameters and equations for the aerothermodynamic performance of the TPS. Since the Orbiter TPS has a low conductivity and most of the heat is radiated, the heating rate at the surface is assumed to be independent of the surface temperature. This implies a one-dimensional thermal model in which heat is only conducted in-depth through the TPS, and that the boundary layer state reaches equilibrium instantaneously (thus the heat rate does not directly depend on the surface temperature upstream). Definition of a film-transfer coefficient is not necessary or desirable at high Mach numbers since the wall temperature is much smaller than the stagnation or adiabatic wall temperature, thus avoiding the introduction of a recovery factor. Therefore, the heat rate or heating model can be calculated and input to the thermal model.

The heating rate depends upon the vehicle trajectory and the atmosphere.[11,12] This dependence is partially accounted for by nondimensionalizing the heat rate by a reference heating rate on a one-foot radius sphere.[1,2] The reference heating ($\dot{q}_r$) for the Orbiter is given by

$$\dot{q}_r = 17700\,\rho_\infty\,(V_\infty/10^4)^{3.07}(1-h_w/h_0) \tag{1a}$$

$$h_w/h_0 = [\dot{q}_r/(\sigma\epsilon)]^{.25}/[T_\infty + \tfrac{1}{2}V_\infty^2/c] \tag{1b}$$

The English Engineering System of units is used, where the heat rate is in BTU/s/ft^2. The ratio of the heating rate ($\dot{q}$) to the reference rate ($\dot{q}_r$) was usually assumed locally to be a linear function of the form

$$\bar{q} = \dot{q}/\dot{q}_r = q_0 + q_\alpha(\alpha-\alpha_0) + q_\beta(\beta-\beta_0) + q_{Re}(Re-Re_0) + q_{\delta e}(\delta_e-\delta_{e0}) + q_{\delta b}(\delta_{bf}-\delta_{bf0}) \tag{2}$$

where q_0 is the magnitude at the reference conditions specified by the zero subscript on each variable. The subscripts on the heating ratio (q) represent partial derivatives or slopes with respect to each variable. Note that the heating model is linear in the parameters. For a short time segment, these parameters are assumed constant. Other functions can be substituted, as long as they are linear in the parameters. Another form of equation which will be used to account for nonlinearity on the elevon is

$$\bar{q} = q_0 + q_\alpha(\alpha-\alpha_0) + \tfrac{1}{2}q_{\alpha\alpha}(\alpha-\alpha_0)^2 + q_{\delta e}(\delta_e-\delta_{e0}) + \tfrac{1}{2}q_{\delta e\delta e}(\delta_e-\delta_{e0})^2 \quad (3)$$

These magnitude and derivative parameters are appropriate for linear estimation.

Once the heat rate to the TPS surface is specified, temperature through the tile can be calculated by the thermal model. A typical TPS cross section for reusable-surface-insulation (RSI) is shown in Fig. 1. The TPS was split into small elements of length (Δx) for a total of L node points. Blocks A through D represent different materials with thermal properties which vary with local temperature and pressure.[4] The convective heat rate ($\dot{q}$) is input to the surface node ($i=1$). The surface radiates heat away and conducts a small amount into the TPS through the thin coating of thickness Δx_A or Δx_1. The surface thermocouple is located at node ($i=2$). The interior of block B with effective thickness (Δx_B) is divided into elements of equal thickness (Δx_i). If additional thermocouples are imbedded, the distance between each is divided into elements of equal thickness so that a node corresponds to the thermocouple location. In block C, the RSI is bonded by room-temperature-vulcanizing (RTV) adhesive to a nomex felt strain-isolation-pad (SIP), which is bonded to the structure by RTV. In Block D, the effective structural thickness and heat sink complete the one-dimensional cross section. An ordinary differential equation for the temperature (U_i) at the ith node point was obtained from an energy balance for each element. A system of L linear differential equations results and is of the form

$$[(c_i\rho_i\Delta x_i + c_{i-1}\rho_{i-1}\Delta x_{i-1})/2]\,U_i = (k_{i-\frac{1}{2}}/\Delta x_{i-1})U_{i-1} - (k_{i-\frac{1}{2}}/\Delta x_{i-1} + k_{i+\frac{1}{2}}/\Delta x_i)U_i + (k_{i+\frac{1}{2}}/\Delta x_i)U_{i+1} - \sigma\epsilon_{i-}(U_i^4 - U_{i-1}^4) - \sigma\epsilon_{i+}(U_i^4 - U_{i+1}^4) + \dot{q}_i \quad (4)$$

Coefficients with subscripts which are less than one or greater than L are zero. The radiation and heat rate terms are zero, except at the surface and backface nodes. The radiation sink temperatures (U_0 and U_{L+1}) are specified at the surface and backface. The emissivities on the side of the element (ϵ_{i+} and ϵ_{i-}) were zero except at the surface, backface, and honeycomb nodes. Given an initial condition (U_I), Eq. (4) can be solved numerically by approximating the time derivative with a first-order backward difference given by

$$\dot{U} = [U(t_n) - U(t_{n-1})]/\nabla t \quad (5)$$

The resulting system of implicit difference equations or matrix equation must be solved simultaneously. The surface-node equation with the nonlinar radiation terms was solved with a Newton-Raphson iteration and extrapolation scheme.[3] A tridiagonal algorithm solved the remaining difference equations.

Numerical solution of Eq. 4 resulted in an accurate simulation of surface and bondline temperature. Time steps and spatial step sizes were reduced to investigate accuracy. A spatial step of 0.00833 ft insured accuracy. Time steps up to one second were acceptable. Larger time steps could be used if transients were not significant.

Estimation of thermal parameters also becomes possible during a transient maneuver. Although numerous parameters could be selected, only parameters which affect the heating derivatives were selected. In addition to the heating parameters, the thermal parameters currently include an effective thermocouple depth or coating thickness (Δx_A), the surface emissivity (ϵ), and a conductivity factor (Φ_B) for the RSI conductivity in block B. A vector of all current parameters (θ) is chosen to be

$$\theta = [q_0\ q_\alpha\ q_\beta\ q_{Re}\ q_{\delta e}\ q_{\delta fb}\ \Delta x_A\ \epsilon\ \Phi_B]^T \quad (6)$$

In subscript form, each parameter is referred to as θ_k. The primary purpose of the heating estimation program is to obtain best estimates of these simulator parameters during transient flight test maneuvers.

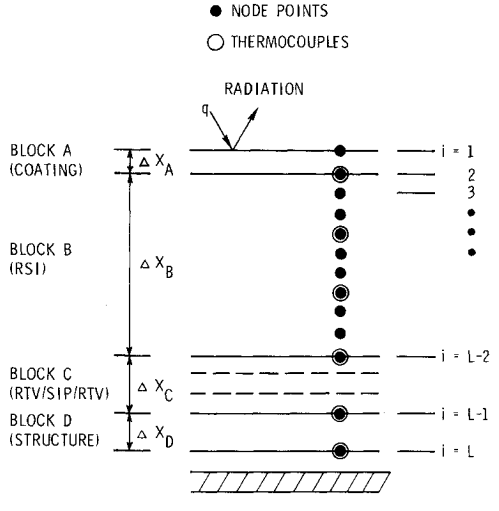

Fig. 1 TPS model cross section.

Parameter Estimation

Parameter estimation is accomplished using system identification theory.[13] Since all states are not measured, best estimates of the temperature at each node are obtained by an extended Kalman filter. Best estimates of parameters are then obtained by maximizing a likelihood function for each parameter. The solution algorithm and program are referred to as HEATEST. A simplified flow diagram for HEATEST is shown in Fig. 2. Each of the blocks will be summarized.

Initial conditions (IC) for HEATEST are required for the solution of Eq. 4 (MODELS block). In addition, initial conditions for the sensitivities and covariance of the temperatures are required. An initial condition for the temperature vector (U) at a time segment start time t_0 is given by

$$U(t_0) = U_I + \tau_I(x) \quad (7)$$

where U_I is the initial temperature vector and the initial error (τ_I) has a covariance matrix P with components

$$P_{ij} = \phi_{ic}^2 U_i(t_0)U_j(t_0)R_{ij} \quad (8)$$

The error model for the stochastic process (τ) was assumed to be stationary and spatially distributed with zero mean and covariance and given by

$$R_{ij} = \exp\left(\sum_{\ell=i}^{j} R_{c\ell}\phi_{tr}\right) \quad (9a)$$

$$R_{c\ell} = \rho_\ell c_\ell \Delta x_\ell^2/k_\ell \quad (9b)$$

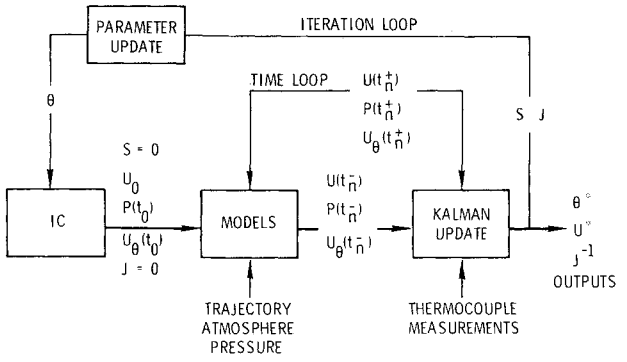

Fig. 2 Simplified HEATEST flow diagram.

The initial model error covariance matrix (Q) uses the same spatial correlation and is given by

$$Q_{ij}=\begin{cases}(\phi_{me}^2+\phi_{bn}^2)R_{ij}U_{EQ}^2 & \text{for } i=j=1\\ \phi^{me}\sqrt{\phi_{me}^2+\phi_{bn}^2}R_{ij}U_{EQ}^2 & \text{for } i=;\neq 1\\ \phi_{me}^2R_{ij}U_{EQ}^2 & \text{for } i\neq j\neq 1\end{cases} \tag{10}$$

where U_{EQ} is an equilibrium temperature calculated from $\dot{q}$, assuming no conduction. The constants ϕ_{tr}, ϕ_{ic}, ϕ_{bn}, and ϕ_{me} are respectively the spatial correlation between nodes, deviation in initial temperatures, deviation in heating rate at the boundary, and deviation in heat flux due to model error.

The initial temperature vector U_I is specified by one of three ways. The temperature distribution is specified by some profile such as a constant based on on-orbit conditions. Initial conditions at the beginning of a time segment may be specified from the output of a previous sequential time segment. The third way, which is more efficient, is based on the radiation equilibrium assumption and an empirically determined R_c time constant. The circuit analogy is used to calculate an equilibrium temperature

$$U_{EQ}(t_n)=gY_1(t_n)-(g-1)Y_1(t_{n-1}) \tag{11a}$$

$$g=1/[1-\exp(-\nabla t/R_c)] \tag{11b}$$

where Y_1 is the surface thermocouple measurement. The heat rate is calculated from the radiation equilibrium temperature U_{EQ} and input to the same algorithm used to propagate temperature (Eq. 4). This procedure works well for generating approximate initial conditions for temperature.

The initial condition for the sensitivity (U_θ) of the temperature of each parameter (θ_k) is assumed to be zero. The θ subscript denotes partial differentation. For sequential time segments, the sensitivities at the end of the previous segment are used.

The temperature, covariance, and sensitivities are propagated to the next time step using differential equations for the TPS (MODELS block). The temperature is propagated by Eq. (4) using the same numerical solution technique as the simulator to obtain an a-priori expectation, $U(t_n^-)$. The minus denotes the expected temperature prior to availability of a measurement, whereas a plus denotes an updated temperature after comparison with a measurement. Differential equations for the sensitivities were derived by taking partial derivatives of Eq. (4) with respect to each parameter (θ_k), and quasilinearizing nonlinear terms. The resulting equations are of the form

$$\dot{U}_{\theta k}=C_kU_{\theta k}+D_k \tag{12}$$

Equation 12 is solved readily for each parameter, since C_k is a tridiagonal matrix. For the covariance, Eq. (4) was first quasilinearized to the form

$$\dot{U}=AU+B+W(t) \tag{13}$$

$W(t)$ has zero mean and a covariance matrix Q. The propagated or a-priori covariance $P(t_n^-)$ was approximated by the difference equation

$$P(t_n^-)=\Phi(\nabla t)P(t_{n-1}^+)\Phi^T(\nabla t)+\int_{t_{n-1}}^{t_n}\Phi(\lambda-t_{n-1})Q\Phi^T(\lambda-t_{n-1})\,d\lambda \tag{14a}$$

$$\Phi(\nabla t)=\exp(A\nabla t) \tag{14b}$$

The transition matrix and integral were originally calculated by Taylor series. A new technique[14] takes advantage of the tridiagonal form of A.

The temperature, covariance, and sensitivities are propagated (MODELS block) until a thermocouple measurement is available. The temperature, covariance, and sensitivities are then updated based on the measurements by the Kalman filter (KALMAN UPDATE block). The location of the total of M thermocouples is identified by the measurement equation

$$Y(t_n)=HU(t_n)+\mu_n \tag{15}$$

H is defined by $H_{mi}=1$ if U_i corresponds to Y_m and $H_{mi}=0$ if U_i does not correspond to Y_m. The error μ_n was assumed to be a white stationary process with zero mean and covariance

$$R_m=\phi_{meas}^2Y_m^2 \tag{16}$$

for each measurement. The constant ϕ_{meas} is related to the deviation in the theromocouple measurement. The updated temperature or a-posterior expectation $U(t_n^+)$ is calculated by

$$U(t_n^+)=U(t_n^-)+GE(t_n) \tag{17a}$$

$$G=P(t_n^-)H^T[H^T[HP(t_n^{-1})H^T+R_m]^{-1} \tag{17b}$$

$$E=Y(t_n)-HU(t_n^-) \tag{17c}$$

The updated covariance and sensitivities are calculated by

$$P(t_n^+)=[I-GH]P(t_n^-)[I-GH]^T+GR_mG^T \tag{18}$$

$$U_{\theta k}(t_n^+)=[I-GH]U_{\theta k}(t_n^-) \tag{19}$$

In summary, the expected temperature, covariance, and sensitivities are propagated (MODELS) for each trajectory and thermocouple sample (TIME LOOP). Updates occur (KALMAN UPDATE) only when a thermocouple measurement is available. This TIME LOOP is continued until the end of the time segment. At the end of a time segment, the parameters (θ_k) are updated (PARAMETER UPDATE). A maximum likelihood criteria was preferred because of experience in estimation of stability derivaties.[6,7] The likelihood function (F) was specified to be the natural logarithm of the joint probability density function of the temperature. The maximum of F was satisfied by equating the gradients to zero. The maximum with respect to U is satisfied by the best estimated temperature

$$U^*=U(t_n^+) \tag{20}$$

if $U(t_n^+)$ is the temperature generated with best estimates of the parameters (θ^*). θ^* is obtained by the gradient algorithm

$$\theta^*=\theta-[\partial^2F/\partial\theta^2]^{-1}\partial F/\partial\theta=\theta+J^{-1}S \tag{21}$$

where J is an approximation assuming a large number of N samples.

$$J = \sum_{n=1}^{N} U_{\theta k}(t_n^-) H^T [HP(t_n^-) H^T + R_m] H U_{\theta k}(t_n^-) \quad (22)$$

The gradient of F is approximated for a large number of N samples by

$$S_k = \sum_{n=1}^{N} U_{\theta k}(t_n^-) H^T [HP(t_n^-) H^T + R_m]^{-1} [Y_n - HU(t_n^-)] \quad (23)$$

Selected parameters are updated by Newton-Raphson iteration. Normally three to five iterations are used for estimates of the parameters. The Cramer-Rao bound is calculated from J^{-1} and provides a measure of the uncertainty in the parameter estimate. After the last PARAMETER UPDATE, the best estimated temperature is obtained by completing the TIME LOOP again. Deviation in the temperature is obtained from the covariance. The average residual error is computed as an indicator of the "match" with the thermocouple data.

Results

Results with two data sources are presented. Thermocouple measurements during transient maneuvers are simulated and distorted with noise and parameter variations.[5] Flight test data specifically from the second and fourth flights (STS-2 and STS-4) were available. Flight results from three locations are presented. These locations include a point off-centerline on the lower surface, the lower outboard elevon, and OMS pod on the upper surface.

Simulated Thermocouple Data

Thermocouple data were simulated for a point on the lower centerline at 75% length ($X/L = .75$). A POPU at Mach 18 and Reynolds number (Re) of two million was simulated. The flow was laminar and the heat rate only a function of α. Data were distorted with 8-bit word resolution and sampled once per second corresponding to the flight recorder.

The simulated surface thermocouple samples and the best estimated temperature from HEATEST at that node are shown in Fig. 3. The estimated heating ratio computed from parameter estimates is compared to the actual simulator model as shown by the circles in Fig. 4. The derivative with respect to the angle of attack (q_α) was changed in the simulator model in Case 2, and the heating ratio successfully estimated, as shown by the triangles. A bias in magnitude (q_0) in Case 3 was correctly estimated, as shown by the squares. Another POPU to lower angle of attack in Case 4 was also estimated correctly, as shown by the diamonds. Thus the program was verified by these cases and by other cases in which errors were introduced.

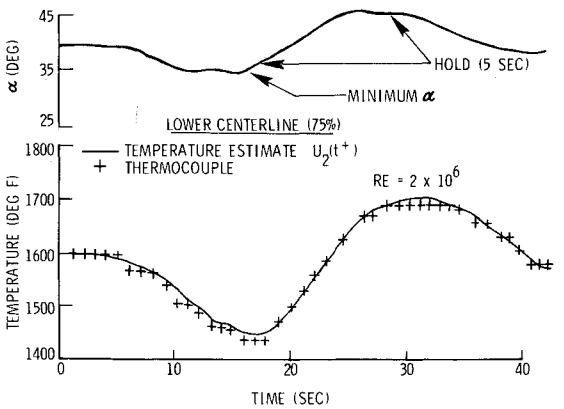

Fig. 3 Simulated thermocouple data with eight-bit word (Mach 18 pushover-pullup maneuver).

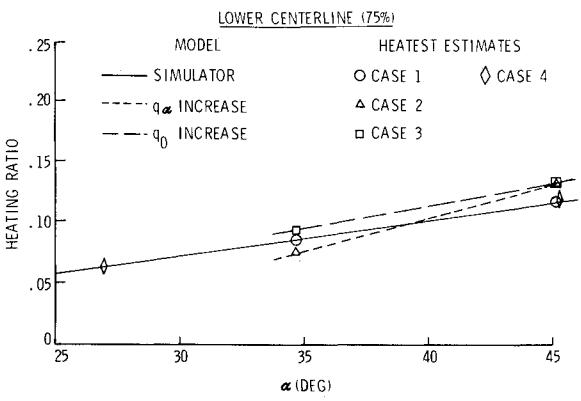

Fig. 4 Heating estimates for simulated thermocouple data at Mach 18.

Lower Surface Flight Thermocouple Data

STS-2 flight thermocouple data at numerous locations on the lower surface were input to HEATEST. Most results have been obtained using only one surface thermocouple.[10] Several locations have multiple thermocouples imbedded through the TPS and are called plugs. A plug is located off-centerline at approximately 70% length ($X/L = .7$) and 10% span ($2y/b = .1$), and has a surface thermocouple and four more imbedded thermocouples. Results can be obtained only for the surface thermocouple or all five thermocouples.

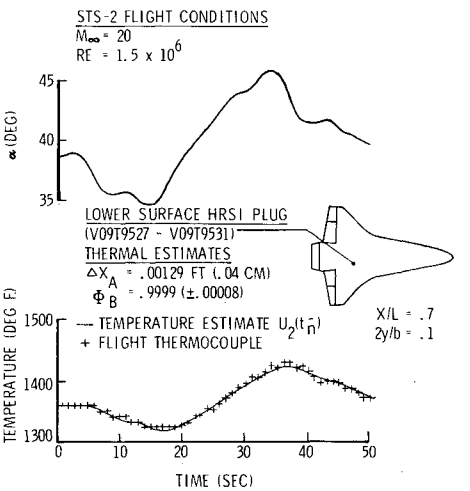

Fig. 5 Lower surface plug STS-2 flight thermocouple data (Mach 20 pushover-pullup maneuver).

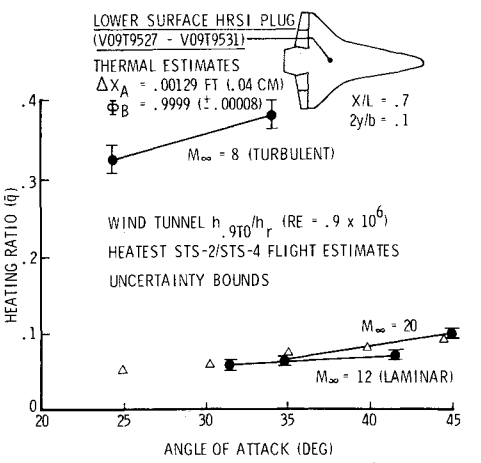

Fig. 6 Heating estimates for lower surface plug from STS-2/STS-4 flight thermocouple data.

Time histories of the angle of attack, surface thermocouple data at the same location, and a-priori temperature during the POPU at Mach 20 and flight Reynolds number of approximately 1.5 million are shown in Fig. 5. As shown in Fig. 5, a good match between a-priori temperature and the surface thermocouple measurements were obtained. The heating estimates are shown in Fig. 6 and compared with wind-tunnel data for laminar flow. Both magnitude and the angle-of-attack derivative agree well. The thermal estimate for effective coating thickness was $\Delta x_A = 0.00129$ ft, which is only slightly higher than the expected value of 0.00125. These estimates were repeated, using only the surface thermocouple for both the test maneuver and the preceding time segment. The same results were obtained, which validates the heating estimation techniques, where only one surface thermocouple measurement is available.

Time histories at the same location for a POPU at Mach 12 during STS-4 are shown in Fig. 7. Telemetered thermocouple data were obtained beginning in the middle of the maneuver.

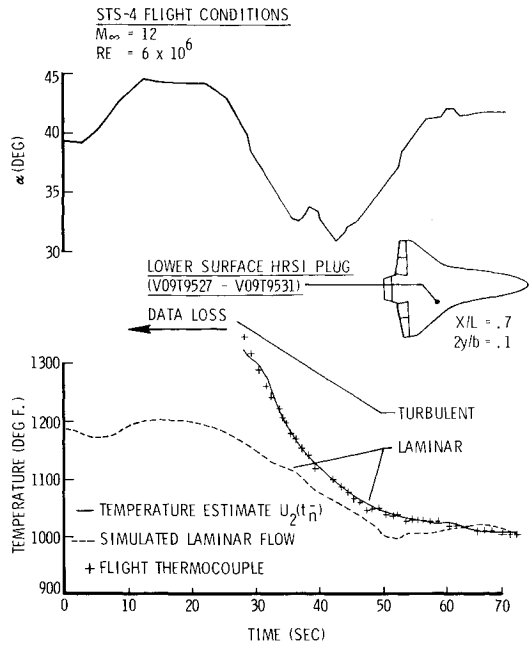

Fig. 7 Lower surface plug STS-4 flight thermocouple data with transition onset during Mach 12 pullup-pushover maneuver.

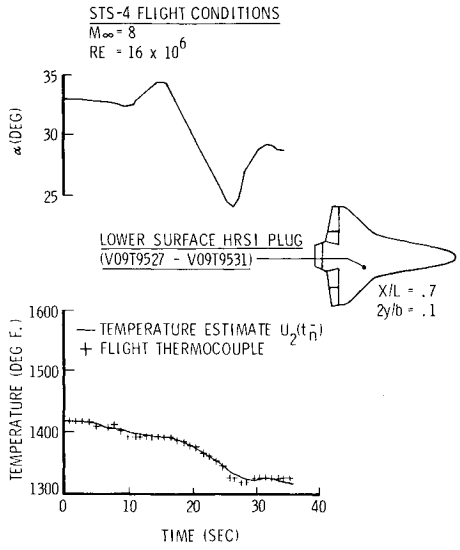

Fig. 8 Lower surface plug STS-4 flight thermocouple data for turbulent flow (Mach 8 pullup-pushover maneuver).

The temperature was unusually high, which indicates transition to turbulent flow during the maneuver. A simulated time history for laminar flow throughout the maneuver is shown. The data show that transition is sensitive to angle of attack at a fairly constant Reynolds number.[10] The flow transitions to turbulent flow and then back to laminar flow when the angle of attack is decreased. After the maneuver, transition occurred at a lower angle of attack, due to a higher Reynolds number.

Heating estimates were obtained for the remaining low angle of attack maneuver and are shown in Fig. 6. The heating magnitude agrees with the laminar data at Mach 20, but with a slightly lower slope. The lower slope could indicate a Mach effect, but could be caused by initial condition error.

Time histories at the same location during a POPU at Mach 8 are shown in Fig. 8. Thermocouple data indicate transition to turbulent flow prior to this maneuver. The maneuver is of short duration and the thermocouple response is barely out of the noise level of the 8-bit data word. Heating estimates were obtained assuming no Reynolds number effect in Fig. 5. The uncertainty bounds are large compared to the laminar estimates.

Control Surface Flight Thermocouple Data

Analysis on the control surface presents a difficult problem, due to numerous variables, to trading between elevon and angle-of-attack derivatives, and to nonlinearity. However, previous results were good on the outboard elevon for the Mach 21 flap maneuer and Mach 20 POPU.[10] Most of the uncertainty seemed to be due to nonlinearity. Because of the nonlinearity, small time segments were required, and in many instances the nonlinearity could not be avoided because of considerable elevon activity. Therefore, a second-order heating model in the elevon deflection angle given by Eq. (3) was used by HEATEST for the flap maneuver and POPU. In addition, the flap maneuvers at Mach 16 and Mach 12 were also analyzed.

STS-2 flight thermocouple measurements on the outboard elevon during the POPU and flap maneuver at Mach 21 were input to HEATEST. Time histories of elevon deflection, angle of attack, thermocouple measurements, and a-priori temperature are shown in Fig. 9. The derivative q_α was fixed at 0.0068 during the flap maneuver because of trading with the elevon derivatives. A long-duration out of trim condition is

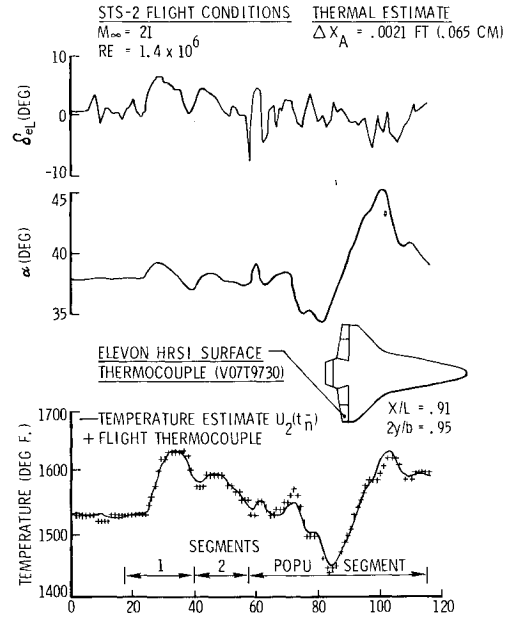

Fig. 9 Lower surface plug STS-4 flight thermocouple (Mach 21 flap maneuver and Mach 20 pushover-pullup maneuver).

needed to distinguish between these derivatives, and this occurs briefly during the POPU. Estimates for the heating during the flap maneuver are shown in Fig. 10. The estimates for the first two time segments at Mach 21 agreed with each other as well as with previous results for the linear heating model and shorter time segments. The uncertainty bound for the lower time segment with the second-order polynomial in δ_e was slightly higher, however. The a-priori temperature still has trouble matching the thermocouple measurements. An angle-of-attack derivative of 0.0068 was estimated, compared to 0.0078 with the first order model, and Δx_A of 0.0021 ft compared with 0.0023. The larger estimates of Δx_A and the difficulty matching the thermocouple measurements suggest that something is not modeled correctly. The increased heating above 5 deg elevon deflection could be transition to turbulence or a local flow phenomenon (flow separation). However, the results provide reasonably accurate estimates based on actual flight data, which are lower than the wind-tunnel data and improve confidence in the ability to expand the envelope of the Orbiter to an aft center of gravity.

STS-2 flight thermocouple measurements at the same location on the elevon during the flap maneuver at Mach 16 were also input to HEATEST. The elevon deflection varied between 0.5 and 3.7 deg, but there was no thermocouple response. The magnitude of the heating agrees with the Mach 21 data as shown in Fig. 10, but the derivative is lower. Expected response to the maneuver was only slightly out of the eight-bit word noise, since the elevon derivative slope is small.

STS-2 flight thermocouple measurements at the same location on the elevon during the flap maneuver at Mach 12 were also input to HEATEST. Time histories are shown in Fig. 11. The flow transitioned to turbulent flow prior to the maneuver. Estimates for the heating for four time segments are shown in Fig. 10. Either the flow is not turbulent at the negative deflection angles or some local flow phenomenon is causing a large nonlinearity in the heating rate. The estimates for the derivative in the first two time segments are believed to be inaccurate. The cause may be related to a combination of initial condition error and the large decrease in heating rate in the second segment. Good estimates were obtained in the third and fourth segments, however. For envelope expansion purposes, the estimates at the large angles in the fourth segment are of primary interest, since the flow is turbulent.

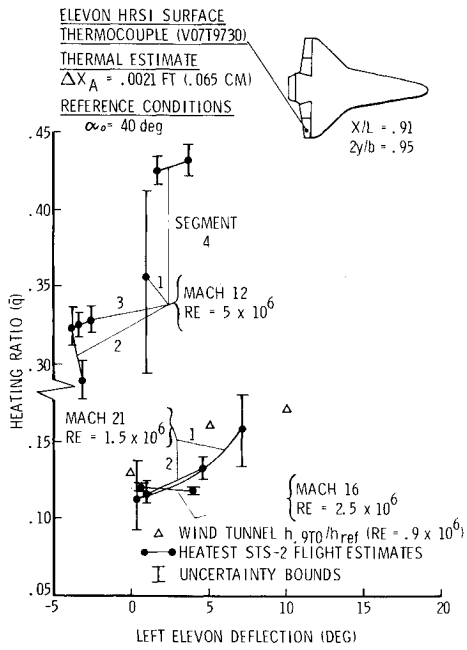

Fig. 10 Heating estimates for outboard elevon from STS-2 flight thermocouple data.

Upper Surface Flight Thermocouple Data

The most significant result of the POPU at Mach 20 during STS-2 was on the side of the OMS pod on the upper surface. A time history of a thermocouple mounted in FRSI on the OMS pod is shown in Fig. 16. The large and unexpected increase in temperature above the design limit was not predicted by the simulator models, based on wind tunnel data at this Reynolds number. Flow impingement on the OMS pod was expected around 30 deg instead of 37 deg, as shown by the negative slope in Fig. 13. Because of nonlinearity, a linear spline was used[15] for Eq. (2) [Eq. (3) did not work]. The depth was

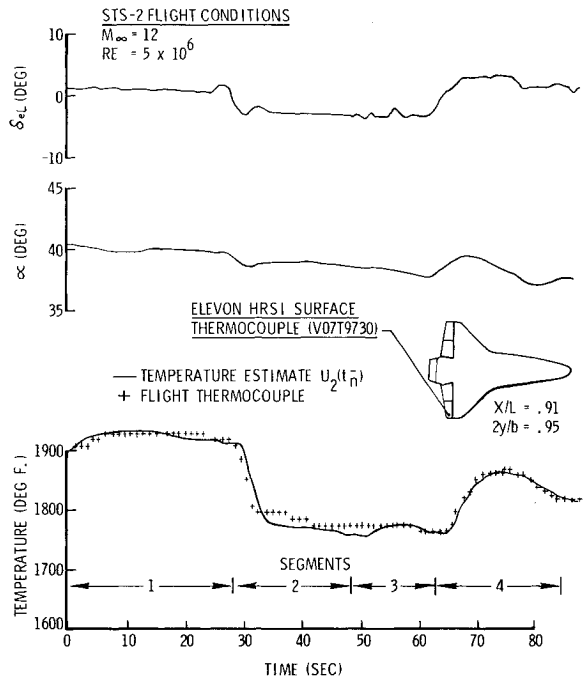

Fig. 11 Outboard elevon STS-2 flight thermocouple data (Mach 21 flap maneuver).

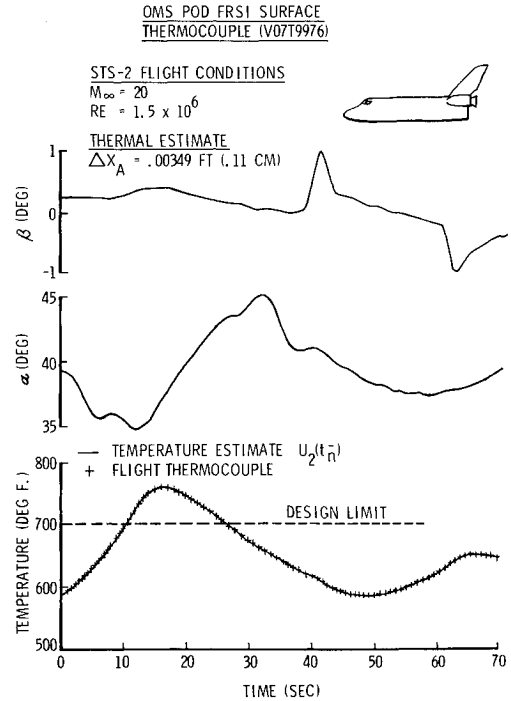

Fig. 12 OMS POD STS-2 flight thermocouple data (Mach 20 pushover-pullup maneuver).

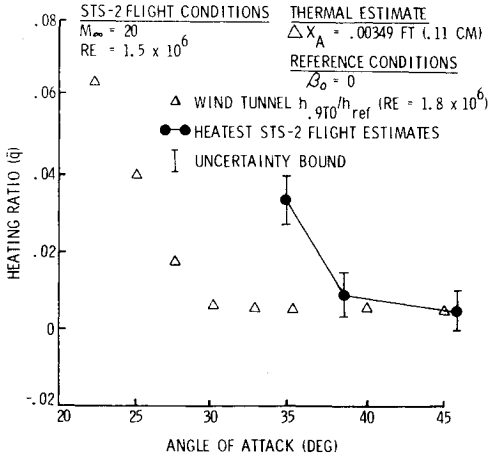

Fig. 13 Heating estimates for OMS POD from STS-2 flight thermocouple data (Mach 20 pushover-pullup maneuver).

estimated[15] to be 0.035 (±.0002) ft. A thick coating was anticipated because of repairs in this area. The side-slip derivative was estimated to be −0.019 (±.004). Uncertainty bounds are fairly large because of complex flow phenomena, and because of upstream wall temperature transients.[8] Therefore, the heating rate is believed valid for transient conditions, but high for steady state.

Although there was concern for the OMS pod before the maneuver, results from the POPU confirm it. The value of transient maneuvers for envelope expansion is demonstrated even without data reduction by examining Fig. 13. With data reduction, a basis for either a placard or redesign of this small area is established.

Conclusions and Recommendations

A parameter-estimation method coupled with an extended Kalman filter has been successfully developed for the reduction of thermocouple data from transient maneuvers. The method was applied to the TPS of the Orbiter for the purpose of safe and rapid expansion of the aerothermodynamic envelope. The method has been applied to simulated thermocouple data, wind tunnel thermocouple data, and flight thermocouple data. The heating at points on the lower surface with surface thermocouples were analyzed easily for laminar flow. For turbulent flow, some difficulty in analyzing Reynolds-number trends was encountered. The heating at control-surface and upper-surface points were analyzed, although some difficulty was encountered because of nonlinear trends in angle-of-attack and deflection angles. The results are useful for mission planning of future operational missions.

The parameter-estimation method should be used in future flight test programs of hypersonic vehicles. The thermocouple instrumentation should be designed for parameter estimation. Special care should be taken to avoid timing errors, the sampling rate should be faster than the thermocouple response, the data resolution should be better than the smallest significant response, and several imbedded thermocouples and a pressure transducer should be located at a point in each critical area.

For envelope expansion, the estimation method is used for data correlation with simulator models. In some cases, data correlation has not worked very well because of lack of sophistication in the heating model (due to flexibility requirements). The heating models can be changed easily as demonstrated by changing reference heating methods and by using a second-order polynomial.

The method is not an inverse technqiue of just generating heating-rate time histories, although it could be. The duration of sequential time segments could be reduced, or the flow diagram could be changed. A parameter estimate could be obtained with the addition of each measurement and based on a prescribed number of previous measurements. Only heating magnitude would be obtained, whereas in the present method, trends in angle of attack and verification of thermal parameters were also obtained.

References

[1]Evans, M.E., "Thermal Boundaries Analysis Program Document," NASA-CR-151025, April 1975.

[2]*Space Shuttle Orbiter Entry Aerodynamic Heating Data Book,* Rockwell International Space Division, Document Number SD73-SH-0184 C. Revision, Books 1 and 2, Oct. 1978.

[3]Williams, S.D. and Curry, D.M., "An Implicit-Iterative Solution of the Heat Conduction Equation with a Radiation Boundary Condition," *International Journal for Numerical Methods in Engineering,* Vol. 11, 1977, pp. 1605-1619.

[4]*Space Shuttle Program Thermodynamic Design Data Book, Thermal Protection Acreage,* Rockwell International Space Division, Document Number SD73-SH-0226, Vol. 2C, Jan. 1981.

[5]Hodge, J.K., Phillips, P.W., and Audley, D.R., "Flight Testing a Manned Lifting Reentry Vehicle (Space Shuttle) for Aerothermodynamic Performance," AIAA Paper 81-2421, Nov. 1981.

[6]Cooke, D.R., "Space Shuttle Stability and Control Flight Test Techniques," AIAA Paper 80-1608, Aug. 1980.

[7]Richardson, D.R. and Kirsten, P.W., "Predicted and Flight Test Results of the Performance and Stability and Control of the Space Shuttle from Reentry to Landing," Paper 3-B, AGARD CP-339, Oct. 1982.

[8]Hodge, J.K., Woo, Y.K., and Cappelano, P.T., "Parameter Estimation for Imbedded Thermocouples in Space Shuttle Wind Tunnel Test Articles with a Nonisothermal Wall," AIAA Paper 83-1533, June 1983.

[9]Audley, D.R. and Hodge, J.K., "Identifying the Aerothermodynamic Environment of the Space Shuttle Orbiter, *Columbia," 6th IFAS Symposium on Identification and System Parameter Estimation,* June 1982.

[10]Hodge, J.K., Audley, D.R., Phillips, P.W., and Hertzler, E.K., "Aerothermodynamic Flight Envelope Expansion for a Manned Lifting Reentry Vehicle (Space Shuttle," Paper 3-A, AGARD CP-339, Oct. 1982.

[11]Price, J.M. and Blanchard, R.C., "Determination of Atmospheric Properties for STS-1 Aerothermodynamics Investigations," AIAA Paper 81-2430, Nov. 1981.

[12]Compton, H.R., Findley, J.T., Kelly, G.M., and Heck, M.L., "Shuttle (STS-1) Entry Trajectory Reconstruction," AIAA Paper 81-2459.

[13]Maybeck, P.S., *Stochastic Models, Estimation and Control,* Academic Press, 1979.

[14]Sagstetter, P.W., "Numerical Computation of the Matrix Riccati Equation for Heat Propagation During Space Shuttle Reentry," Master's Thesis (AFIT/GCS/MA/82D-7), Air Force Institute of Technology, Wright-Patterson Air Force Base, OH.

[15]Lutes, C.D., "Nonlinear Modeling and Initial Condition Estimation for Identifying the Aerothermodynamic Environment of the Space Shuttle Orbiter," Master's Thesis (AFIT/GAE/AA/83D-14), Air Force Institute of Technology, Wright-Patterson Air Force Base, OH.